

# Lambda production in central Pb+Pb collisions at CERN-SPS energies

**A. Mischke for the NA49 Collaboration**

Gesellschaft für Schwerionenforschung, D-64291 Darmstadt, Germany

E-mail: a.mischke@gsi.de

S.V. Afanasiev<sup>9</sup>, T. Anticic<sup>20</sup>, D. Barna<sup>5</sup>, J. Bartke<sup>7</sup>, R.A. Barton<sup>3</sup>, L. Betev<sup>10</sup>, H. Bialkowska<sup>17</sup>, A. Billmeier<sup>10</sup>, C. Blume<sup>8</sup>, C.O. Blyth<sup>3</sup>, B. Boimska<sup>17</sup>, M. Botje<sup>1</sup>, J. Bracinik<sup>4</sup>, R. Bramm<sup>10</sup>, R. Brun<sup>11</sup>, P. Bunčić<sup>10,11</sup>, V. Cerny<sup>4</sup>, J.G. Cramer<sup>19</sup>, P. Csató<sup>5</sup>, P. Dinkelaker<sup>10</sup>, V. Eckardt<sup>16</sup>, P. Filip<sup>16</sup>, H.G. Fischer<sup>11</sup>, Z. Fodor<sup>5</sup>, P. Foka<sup>8</sup>, P. Freund<sup>16</sup>, V. Friese<sup>15</sup>, J. Gál<sup>5</sup>, M. Gaździcki<sup>10</sup>, G. Georgopoulos<sup>2</sup>, E. Gładysz<sup>7</sup>, S. Hegyi<sup>5</sup>, C. Höhne<sup>15</sup>, G. Igo<sup>14</sup>, P.G. Jones<sup>3</sup>, K. Kadija<sup>11,20</sup>, A. Karev<sup>16</sup>, V.I. Kolesnikov<sup>9</sup>, T. Kollegger<sup>10</sup>, M. Kowalski<sup>7</sup>, I. Kraus<sup>8</sup>, M. Krepes<sup>4</sup>, M. van Leeuwen<sup>1</sup>, P. Lévai<sup>5</sup>, A.I. Malakhov<sup>9</sup>, S. Margetis<sup>13</sup>, C. Markert<sup>8</sup>, B.W. Mayes<sup>12</sup>, G.L. Melcumov<sup>9</sup>, J. Molnár<sup>5</sup>, J.M. Nelson<sup>3</sup>, G. Pál<sup>5</sup>, A.D. Panagiotou<sup>2</sup>, K. Perl<sup>18</sup>, A. Petridis<sup>2</sup>, M. Pikna<sup>4</sup>, L. Pinsky<sup>12</sup>, F. Pühlhofer<sup>15</sup>, J.G. Reid<sup>19</sup>, R. Renfordt<sup>10</sup>, W. Retyk<sup>18</sup>, C. Roland<sup>6</sup>, G. Roland<sup>6</sup>, A. Rybicki<sup>7</sup>, T. Sammer<sup>16</sup>, A. Sandoval<sup>8</sup>, H. Sann<sup>8</sup>, N. Schmitz<sup>16</sup>, P. Seyboth<sup>16</sup>, F. Siklér<sup>5</sup>, B. Sitar<sup>4</sup>, E. Skrzypczak<sup>18</sup>, G.T.A. Squier<sup>3</sup>, R. Stock<sup>10</sup>, H. Ströbele<sup>10</sup>, T. Susa<sup>20</sup>, I. Szentpétery<sup>5</sup>, J. Sziklai<sup>5</sup>, T.A. Trainor<sup>19</sup>, D. Varga<sup>5</sup>, M. Vassiliou<sup>2</sup>, G.I. Veres<sup>5</sup>, G. Vesztegombi<sup>5</sup>, D. Vranić<sup>8</sup>, S. Wenig<sup>11</sup>, A. Wetzler<sup>10</sup>, C. Whitten<sup>14</sup>, I.K. Yoo<sup>15</sup>, J. Zaraneck<sup>10</sup>, J. Zimányi<sup>5</sup>

<sup>1</sup>NIKHEF, Amsterdam, Netherlands.

<sup>2</sup>Department of Physics, University of Athens, Athens, Greece.

<sup>3</sup>Birmingham University, Birmingham, England.

<sup>4</sup>Comenius University, Bratislava, Slovakia.

<sup>5</sup>KFKI Research Institute for Particle and Nuclear Physics, Budapest, Hungary.

<sup>6</sup>MIT, Cambridge, USA.

<sup>7</sup>Institute of Nuclear Physics, Cracow, Poland.

<sup>8</sup>Gesellschaft für Schwerionenforschung (GSI), Darmstadt, Germany.

<sup>9</sup>Joint Institute for Nuclear Research, Dubna, Russia.

<sup>10</sup>Fachbereich Physik der Universität, Frankfurt, Germany.

<sup>11</sup>CERN, Geneva, Switzerland.

<sup>12</sup>University of Houston, Houston, TX, USA.

<sup>13</sup>Kent State University, Kent, OH, USA.

<sup>14</sup>University of California at Los Angeles, Los Angeles, USA.

<sup>15</sup>Fachbereich Physik der Universität, Marburg, Germany.

<sup>16</sup>Max-Planck-Institut für Physik, Munich, Germany.

<sup>17</sup>Institute for Nuclear Studies, Warsaw, Poland.

<sup>18</sup>Institute for Experimental Physics, University of Warsaw, Warsaw, Poland.

<sup>19</sup>Nuclear Physics Laboratory, University of Washington, Seattle, WA, USA.

<sup>20</sup>Rudjer Boskovic Institute, Zagreb, Croatia.

### Abstract.

In this paper we present recent results from the NA49 experiment for  $\Lambda$  and  $\bar{\Lambda}$  hyperons produced in central Pb+Pb collisions at 40, 80 and 158 A·GeV. Transverse mass spectra and rapidity distributions for  $\Lambda$  are shown for all three energies. The shape of the rapidity distribution becomes flatter with increasing beam energy. The multiplicities at mid-rapidity as well as the total yields are studied as a function of collision energy including AGS measurements. The ratio  $\Lambda/\pi$  at mid-rapidity and in  $4\pi$  has a maximum around 40 A·GeV. In addition,  $\bar{\Lambda}$  rapidity distributions have been measured at 40 and 80 A·GeV, which allows to study the  $\bar{\Lambda}/\Lambda$  ratio.

Submitted to: *J. Phys. G: Nucl. Phys.*

PACS numbers: appear here

## 1. Introduction

Relativistic nucleus-nucleus collisions allow the investigation of nuclear matter at high temperatures and densities. In-medium production of strangeness in nucleus-nucleus collisions is expected to differ from what is known from elementary hadron-hadron interactions. The measurement of strange baryons like  $\Lambda$ (uds) hyperons, which contain between 25 and 60% of the total strangeness produced (depending on the energy), offer the possibility to study simultaneously strangeness production and the effect of baryon density in A-A collisions. The excitation function of hyperon production will probe the behavior of strange baryons at various energy densities in the interaction zone, which depend on the collision energy. The NA49 collaboration contributes to the excitation function the measurements of  $\Lambda$  and  $\bar{\Lambda}$  hyperons in central Pb+Pb collisions at 40, 80 and 158 A·GeV.

## 2. The NA49 experiment at CERN-SPS

The experiment NA49 is a large acceptance hadron spectrometer at the CERN-SPS (figure 1). Tracking and particle identification by the measurement of the specific energy loss ( $dE/dx$ ) is performed by two Time Projection Chambers (VTPC-1 and VTPC-2) located inside two vertex magnets (1.5 and 1.1 T, respectively) and two large volume TPC's (MTPC-L and MTPC-R) situated downstream of the magnets symmetrically to the beam line [1]. The relative  $dE/dx$  resolution is 3-4 % and the momentum resolution

$\frac{\sigma(p)}{p^2} = 0.3 \cdot 10^{-4}(\text{GeV}/c)^{-1}$ . Two Time-of-Flight walls (TOF-TL and TOF-TR) give additional particle identification near mid-rapidity. The trigger on centrality is based on the energy measurement in the forward calorimeter (VCAL), which detects the projectile spectator nucleons.

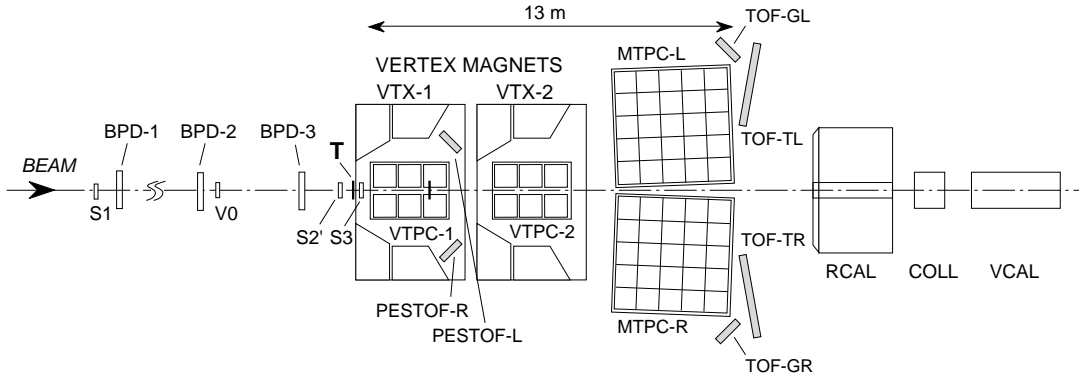


**Figure 1:** Schematic arrangement of the experiment NA49 [1]. For details see text.

### 3. $\Lambda$ production

The NA49 collaboration has taken central Pb+Pb data at 40, 80 and 158 GeV per nucleon. For the present analysis, the 7 % most central interactions at 40 and 80 A·GeV were selected. The resulting event sample has 349 participating nucleons on average. For 158 A·GeV the trigger selected the 10 % most central events (335 participants). The number of analyzed events is 400k for 40 and 158 A·GeV as well as 300k for 80 A·GeV.  $\Lambda$  and  $\bar{\Lambda}$  hyperons are identified by reconstructing their decay topologies  $\Lambda \rightarrow p + \pi^-$  and  $\bar{\Lambda} \rightarrow \bar{p} + \pi^+$ , respectively, with a branching fraction of 63.9%. The charged decay products are measured with the TPC's. In figure 2, the invariant mass distributions are shown for all three energies. Clear signals are observed with reasonable signal-to-background ratios. The agreement between the measured masses and the nominal value, indicated by the arrows, is excellent. The mass resolution is  $2 \text{ MeV}/c^2$  ( $\sigma_m$ ). The signals were extracted after subtracting the background, which is well described by a third-order polynomial. The average numbers of  $\Lambda$  reconstructed are also shown in the figures.

#### 3.1. Spectra

We have performed corrections bin by bin in rapidity and transverse momentum for geometrical acceptance and tracking efficiency using a full Monte Carlo simulation of the detector in GEANT. The reconstruction efficiency was obtained by embedding GEANT simulated  $\Lambda$  in raw data events (one per event) followed by the same reconstruction procedure, which was used for the normal data sample. The transverse mass ( $m_T = \sqrt{p_T^2 + m_0^2}$ , where  $m_0$  is the rest mass of the particle) distributions of  $\Lambda$  (at mid-rapidity)

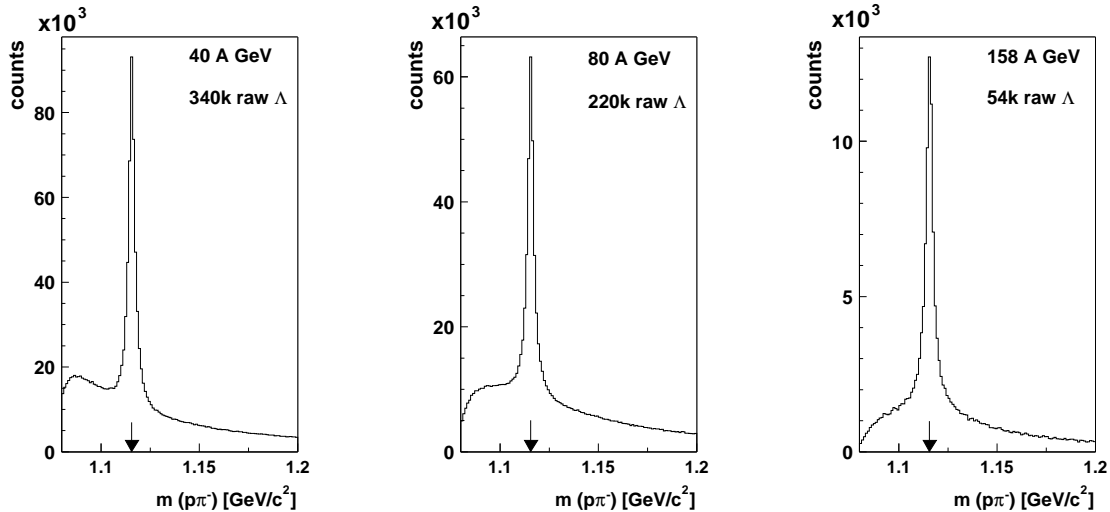


**Figure 2:** The invariant mass distributions of  $p\text{-}\pi^-$  pairs in central Pb+Pb reactions at 40 (left), 80 (middle) and 158 GeV per nucleon (right). The measured masses are in good agreement with the PDG value of  $1.115 \text{ GeV}/c^2$ , indicated by the arrows. The mass resolution is  $2 \text{ MeV}/c^2$  for all three energies.

are plotted in figure 3. All spectra follow a single exponential function in  $m_T$  according to

$$\frac{1}{m_T} \frac{d^2n}{dm_T dy} \propto e^{-\frac{m_T}{T}},$$

where  $T$  is the inverse slope parameter. The slope factors are fitted in the interval  $0.2 \text{ GeV}/c^2 \leq m_T \leq 1.6 \text{ GeV}/c^2$  resulting in  $T = (290 \pm 16) \text{ MeV}$  at 158 A·GeV,  $T = (269 \pm 19) \text{ MeV}$  at 80 A·GeV and  $T = (252 \pm 15) \text{ MeV}$  at 40 A·GeV. The slope parameter increases with increasing energy. This is illustrated in figure 4, where the inverse slope  $T$  is shown as a function of center-of-mass energy per nucleon nucleon pair,  $\sqrt{s}$ . The value published by the WA97 collaboration at 158 A·GeV [2] and the preliminary result from the STAR collaboration (central Au+Au at  $\sqrt{s}=130 \text{ GeV}$  [3]) as well as an estimate of the slope at AGS energies [4] confirm the trend seen in our data. Another estimate at AGS beam energies [5] seems to be too high but still compatible due to its large errors.

At 40 and 80 A·GeV the acceptance covers the full transverse momentum region down to  $p_T = 0 \text{ GeV}/c$ . The yield in each rapidity bin is the integral of the  $p_T$ -distribution. At 158 A·GeV, however, an extrapolation using the fitted slope parameter is necessary to determine the yield (extrapolation factor = 1.22). Feeddown corrections for cascade decays are not applied, but these corrections are expected to be small. The resulting rapidity distributions for all three energies are compared in figure 5. The baseline for 40 A·GeV is at 0, indicated by the horizontal line. For clearness, the baseline for 80 and 158 A·GeV is shifted by 10 and 20, respectively. The reflected points (open circles) are close to the measured ones (filled circles). At 40 A·GeV the produced  $\Lambda$  are concentrated at mid-rapidity, whereas the distribution becomes flatter at higher energies.

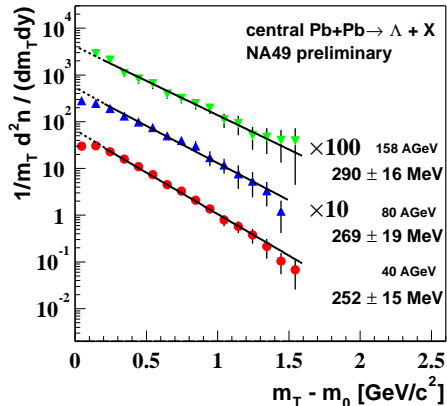


**Figure 3:** A summary of the transverse mass spectra for all three energies. The fitted inverse slope parameter increases with increasing energy.

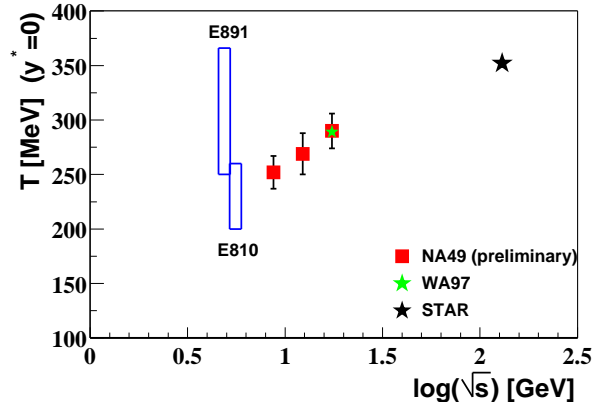


**Figure 4:** The inverse slope parameter  $T$  as a function of the beam energy. The open rectangular symbols are estimates of  $T$ . A slight increase with energy is observed. Note the suppressed zero.

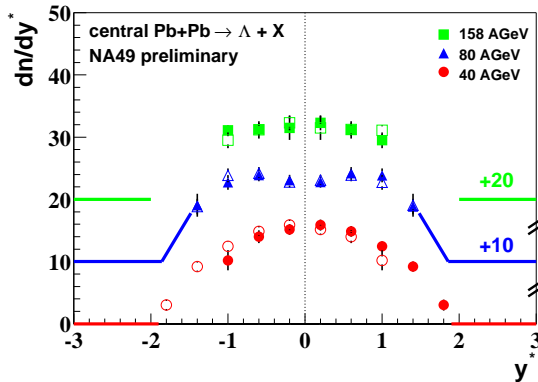


**Figure 5:** The rapidity distributions of  $\Lambda$  hyperons in central Pb+Pb collisions at 40, 80 and 158 A-GeV. The baseline for 80 and 158 A-GeV is shifted by 10 and 20 units, respectively.

### 3.2. Energy dependence

The maximum of the  $\Lambda$  rapidity distribution decreases with increasing collision energy, as shown in figure 5. This is highlighted in figure 6 (left), where the yield at mid-rapidity ( $y^*=0$ ) is plotted as a function of c.m. energy, including measurements from AGS energies [5] [6] and from the WA97 collaboration [7]. The rapidity density  $\frac{dn}{dy}(y^*=0)$  steeply increases at low energies and reaches its maximum at or below 40 A-GeV. In the ratio  $\Lambda/\pi$  (see figure 6 right) this effect is even enhanced. The pion multiplicity is calculated in the form  $\pi = 1.5 \cdot (\pi^+ + \pi^-)$ , using measurements from [8] and assuming isospin symmetry of the interacting nuclei. The ratio  $\Lambda/\pi$  shows a steep increase at AGS energies and a strong drop at SPS energies. Much further on the energy scale, at  $\sqrt{s}=130$  GeV, the first result from the STAR collaboration [3], indicated by the arrow, fits smoothly into this systematics. The strong non-monotonic energy behavior is explained by the superposition of the slightly decreasing  $\Lambda$  yield and the increasing  $\pi$  yield in the range of SPS energies.

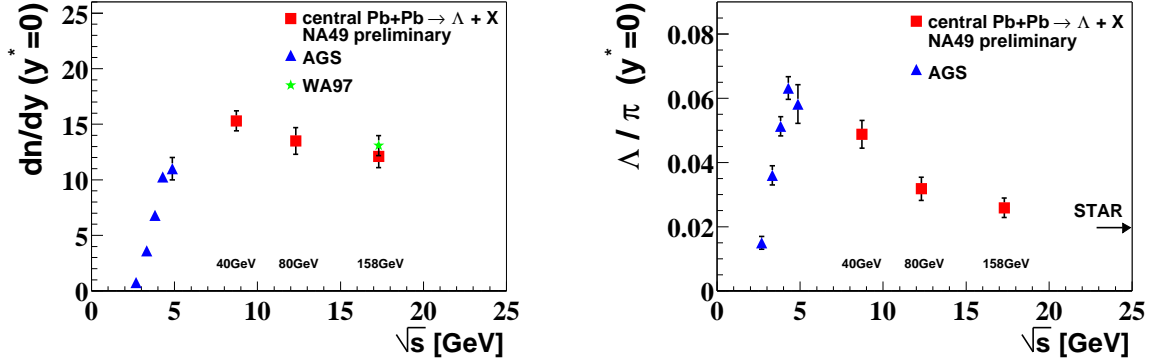


**Figure 6:** (left) The rapidity density as a function of c.m. energy. (right) The energy dependence of the  $\Lambda/\pi$  ratio (at mid-rapidity). For comparison, AGS measurements are also shown. The first result from the STAR collaboration [3], measured at  $\sqrt{s}=130$  GeV, is illustrated with a horizontal arrow.

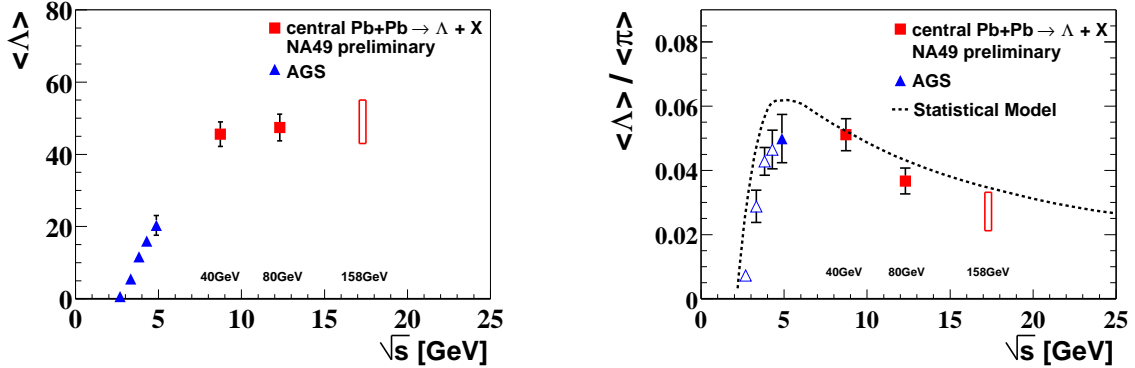


**Figure 7:** The total  $\Lambda$  multiplicity (left) and the ratio of total  $\Lambda$  and  $\pi$  yields (right) as a function of c.m. energy for central Pb+Pb collisions. The dotted line is a statistical model calculation by [14].

The large acceptance of the NA49 detector allows to study also the particle yields in the full phase space, as illustrated in figure 5. The total yields are obtained by integration of  $\frac{dn}{dy}$  with only small extrapolations into unmeasured regions at 40 and 80 A·GeV. For 158 A·GeV the rapidity distribution must be extrapolated, using realistic estimates of the tails of the  $\frac{dn}{dy}$  distribution, e.g. those of the net-proton distribution at 158 A·GeV [9] or the  $\Lambda$  rapidity distribution in central S+S collisions [10]. In figure 7 (left), the total multiplicities as well as the AGS measurements [11] [12] are summarized. The total  $\Lambda$  multiplicity increases in the AGS region and saturates at SPS energies. The  $\langle N_{\Lambda} \rangle / \langle N_{\pi} \rangle$  ratio (the pion yields are taken from [8]) follows a non-monotonic energy dependence (see figure 7 right).

The non-monotonic behavior of the strangeness-to-entropy ratio is predicted to occur in the case of deconfinement [13]. The  $\langle N_{\Lambda} \rangle / \langle N_{\pi} \rangle$  ratio is sensitive to the strangeness-to-entropy ratio and in addition to the baryon density. The effect of baryon density is strong as shown in figure 7 (right), where our results are compared with statistical model calculations by [14], which are represented by the dotted line. The curve lies systematically above the measured points.

#### 4. $\bar{\Lambda}$ production at 40 and 80 A·GeV

A full analysis, as described in section 3.1., was also performed for  $\bar{\Lambda}$  hyperons. The resulting rapidity spectra are illustrated in figure 8. The filled circles represent the measured points and the open circles indicate the points reflected with respect to mid-rapidity. Both distributions show a maximum at mid-rapidity with a rapidity density of  $0.42 \pm 0.03$  and  $1.06 \pm 0.1$  for 40 and 80 A·GeV, respectively. The width of a Gaussian fitted to the distribution gives  $\sigma_y = 0.71 \pm 0.05$  at 40 and  $\sigma_y = 0.90 \pm 0.13$  at 80 A·GeV. The integrated  $4\pi$  yields are  $0.74 \pm 0.06$  and  $2.26 \pm 0.35$   $\bar{\Lambda}$  per event for 40 and 80 A·GeV, respectively. This means that the rapidity distribution becomes broader going from 40 to 80 A·GeV and the maximum increases by a factor of about 2.5.

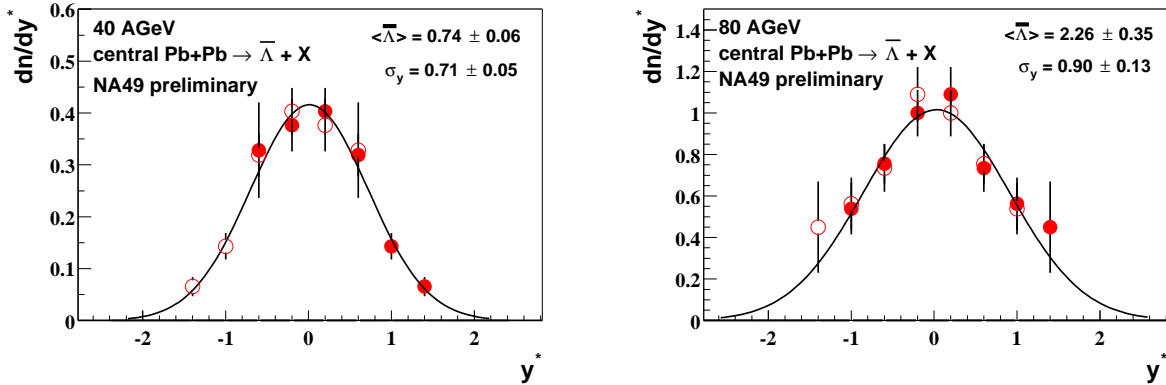


**Figure 8:** The rapidity distribution of  $\bar{\Lambda}$  hyperons produced in central Pb+Pb collisions at 40 (left) and 80 A·GeV (right).

The  $\bar{\Lambda}/\Lambda$  ratio is studied at mid-rapidity as well as over the full rapidity range. At mid-rapidity this ratio is extracted to be  $\bar{\Lambda}/\Lambda = 0.025 \pm 0.0023$  at 40 A·GeV, which is in good agreement with  $0.023 \pm 0.001$  (uncorrected yields of  $\Lambda$  and  $\bar{\Lambda}$ ) measured by the WA97 collaboration [15], and  $\bar{\Lambda}/\Lambda = 0.079 \pm 0.01$  at 80 A·GeV. The  $4\pi$  ratios are found to be  $0.016 \pm 0.0018$  and  $0.048 \pm 0.005$  for 40 and 80 A·GeV, respectively. We deduce from these numbers that the ratio  $\bar{\Lambda}/\Lambda$  increases by a factor of 3, at mid-rapidity and  $4\pi$ , when going from 40 to 80 A·GeV. That implies a reduction of the baryon chemical potential  $\mu_B$  of about 27%.

#### 5. Summary and outlook

Within the framework of the NA49 energy scan program  $\Lambda$  and  $\bar{\Lambda}$  hyperons were measured at 158 A·GeV and for the first time at 40 and 80 A·GeV over a large range of rapidity and transverse momentum. The inverse slope parameter near mid-rapidity seems to increase slightly with increasing energy. This indicates the effect of transverse flow which is expected to increase with collision energy. The rapidity density at mid-rapidity decreases with increasing energy in the SPS energy range. The  $\Lambda/\pi$  ratio shows a significant non-monotonic energy dependence. The  $\bar{\Lambda}$  rapidity distribution at

80 A·GeV is observed to be broader than at 40 A·GeV and the total multiplicity increases by a factor of 3. The  $\bar{\Lambda}/\Lambda$  ratio increases by a factor of 3, at mid-rapidity and  $4\pi$ , when going from 40 to 80 A·GeV. The planned 20 and 30 A·GeV run in the year 2002 will cover the interesting range between top AGS and low SPS energies.

## Acknowledgements

This work was supported by the Director, Office of Energy Research, Division of Nuclear Physics of the Office of High Energy and Nuclear Physics of the US Department of Energy (DE-ACO3-76SFOOO98 and DE-FG02-91ER40609), the US National Science Foundation, the Bundesministerium für Bildung und Forschung, Germany, the Alexander von Humboldt Foundation, the UK Engineering and Physical Sciences Research Council, the Polish State Committee for Scientific Research (5 P03B 13820 and 2 P03B 02418), the Hungarian Scientific Research Foundation (T14920 and T23790), the EC Marie Curie Foundation, and the Polish-German Foundation.

## References

- [1] S.V. Afanasiev *et al.* [NA49 Collaboration], Nucl. Instrum. Meth. **A430** (1999) 210.
- [2] F. Antinori *et al.* [WA97 Collaboration], Eur. Phys. J. **C14** (1999) 633.
- [3] S. Margetis and G. van Buren,  
*Workshop on Thermalization and Chemical Equilibration in Heavy Ions Collisions at RHIC*,  
 20.-21. Juli 2001, <http://connery.star.bnl.gov/thermalfest/program.html>.
- [4] S.E. Eiseman *et al.* [E810 Collaboration], Phys. Lett. **B297** (1992) 44-48.
- [5] S. Ahmad *et al.* [E891 Collaboration], Phys. Lett. **B382** (1996) 35-39.
- [6] G. Rai *et al.* [E895 Collaboration], *Latest Results from the AGS E895 experiment*,  
 QM99 (Torino), <http://www.qm99.to.infn.it/rai/ri11.html>.
- [7] E. Andersen *et al.* [WA97 Collaboration], Phys. Lett. **B449** (1999) 401-406.
- [8] J.L. Klay, PhD thesis, University of California, Davis (2001), Phys. Rev. **C**: in preparation.  
 L. Ahle *et al.* [E802 Collaboration], Phys. Rev. **C57** (1998) 466.  
 L. Ahle *et al.* [E866 Collaboration and E917 Collaboration], Phys. Lett. **B476** (2000) 1.
- [9] H. Appelshäuser *et al.* [NA49 Collaboration], Phys. Rev. Lett. **82** (1999) 2471.
- [10] T. Alber *et al.* [NA35 Collaboration] Z. Phys. **C64** (1994) 195-207
- [11] C. Pinkenburg *et al.* [E895 Collaboration], QM2001 proceedings, Nucl. Phys. **A698** (2002) 495c-498c.
- [12] F. Becattini, J. Cleymans, A. Keränen, E. Suhonen, K. Redlich, Phys. Rev. **C64**, (2001), 024901 (hep-ph/0002267).
- [13] M. Gaździcki and M.I. Gorenstein, Acta Phys. Polon. **B30** (1999) 2705 (hep-ph/9803462).
- [14] P. Braun-Munzinger, J. Cleymans, H. Oeschler, K. Redlich, Nucl. Phys. **A697** (2002) 902-912 (hep-ph/0106066).
- [15] N. Carrer *et al.* [WA97/NA57 Collaboration], QM2001 proceedings, Nucl. Phys. **A698** (2002) 118c-126c.